ACS Pharmacology & Translational Science

pubs.acs.org/ptsci

Article

Small Molecule Targeting of Oxysterol-Binding Protein (OSBP)-Related Protein 4 and OSBP Inhibits Ovarian Cancer Cell Proliferation in Monolayer and Spheroid Cell Models

Ryan C. Bensen,[#] Gokhan Gunay,[#] Matthew C. Finneran, Isha Jhingan, Handan Acar,[*] and Anthony W. G. Burgett[*]

Cite This: *ACS Pharmacol. Transl. Sci.* 2021, 4, 744−756

Read Online

ACCESS | Metrics & More | Article Recommendations | Supporting Information

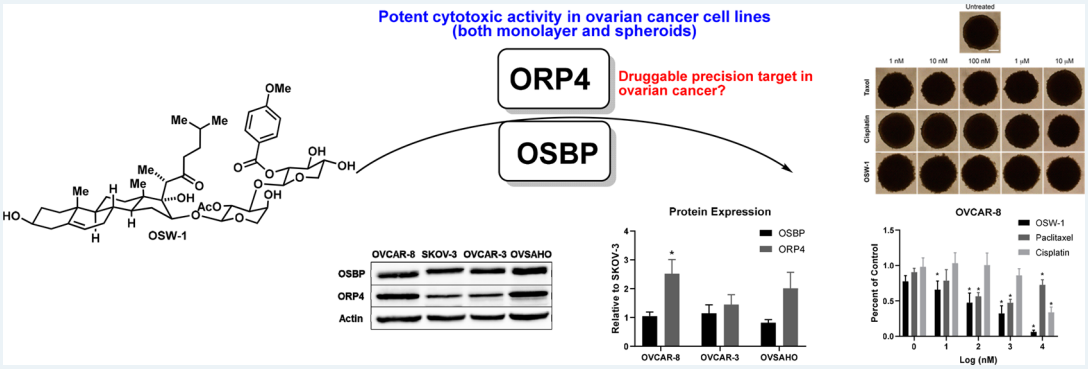

ABSTRACT: The development of precision drugs for the selective treatment of ovarian cancer will require targeting proliferative factors selectively expressed in ovarian tumors or targeting unique physiological microenvironments specific for ovarian tumors. Here, we report that oxysterol-binding protein (OSBP)-related protein 4 (ORP4) is a potential druggable precision target in ovarian cancer cells. ORP4 has limited expression in normal tissues and was recently recognized to be a cancer-specific driver of cellular proliferation, including in patient-isolated leukemias. We demonstrate that ORP4 is strongly expressed in a panel of ovarian cancer cell lines. The antiproliferative natural product compound OSW-1 targets ORP4 and OSBP. Our results demonstrate that the OSW-1 compound has high antiproliferative potency in both monolayer and three-dimensional ovarian cancer spheroid models, especially compared to the standard-of-care agents cisplatin and paclitaxel. OSW-1 compound treatment induces a loss of ORP4 expression after 48 h, which is coincident with the cytotoxic effects of OSW-1. The absence of extracellular lipids markedly potentiated the cytotoxicity of OSW-1, which was reversed by addition of extracellular free cholesterol. OSBP, but not ORP4, is reported to transport cholesterol and other lipids between organelles. Our results indicate that the targeting of ORP4 is responsible for the antiproliferative activity of the OSW-1 compound, but that in the absence of exogenously supplied cholesterol, which might be similar to the *in vivo* ovarian cancer microenvironment, possible OSW-1 targeting of OSBP further potentiates the anticancer activity of the compound. Overall, ORP4 and potentially OSBP are revealed as potential druggable targets for the development of novel treatments for ovarian cancer.

KEYWORDS: *precision anticancer drug development, OSBP, ORP4, OSW-1, ovarian cancer*

Ovarian cancer is the deadliest gynecological malignancy, causing over 14 000 deaths per year in the United States.[1] With a 50% five-year survival rate, the high morbidity and mortality of ovarian cancer is due to diagnosis commonly occurring after the metastatic spread of the cancer (stage III or IV), at which point the treatment options have limited efficacy.[2] The major, and most serious, type of epithelial ovarian cancer (EOC) is high-grade serous carcinoma (HGSC).[3] Standard of care (SOC) treatment of metastatic HGSC is a combination chemotherapy of a platinum-based drug (e.g., cisplatin or carboplatin) and an antimitotic agent (e.g., paclitaxel).[4] HGSC malignancies are complicated due to an atypical route of metastasis and the complex heterogeneity of the tumors.[3] Unlike most epithelial cancers, HGSC disseminates mainly through a transcoelomic route rather than a hematogenous or lymphatic route.[3] The transcoelomic

Received: December 6, 2020
Published: February 4, 2021

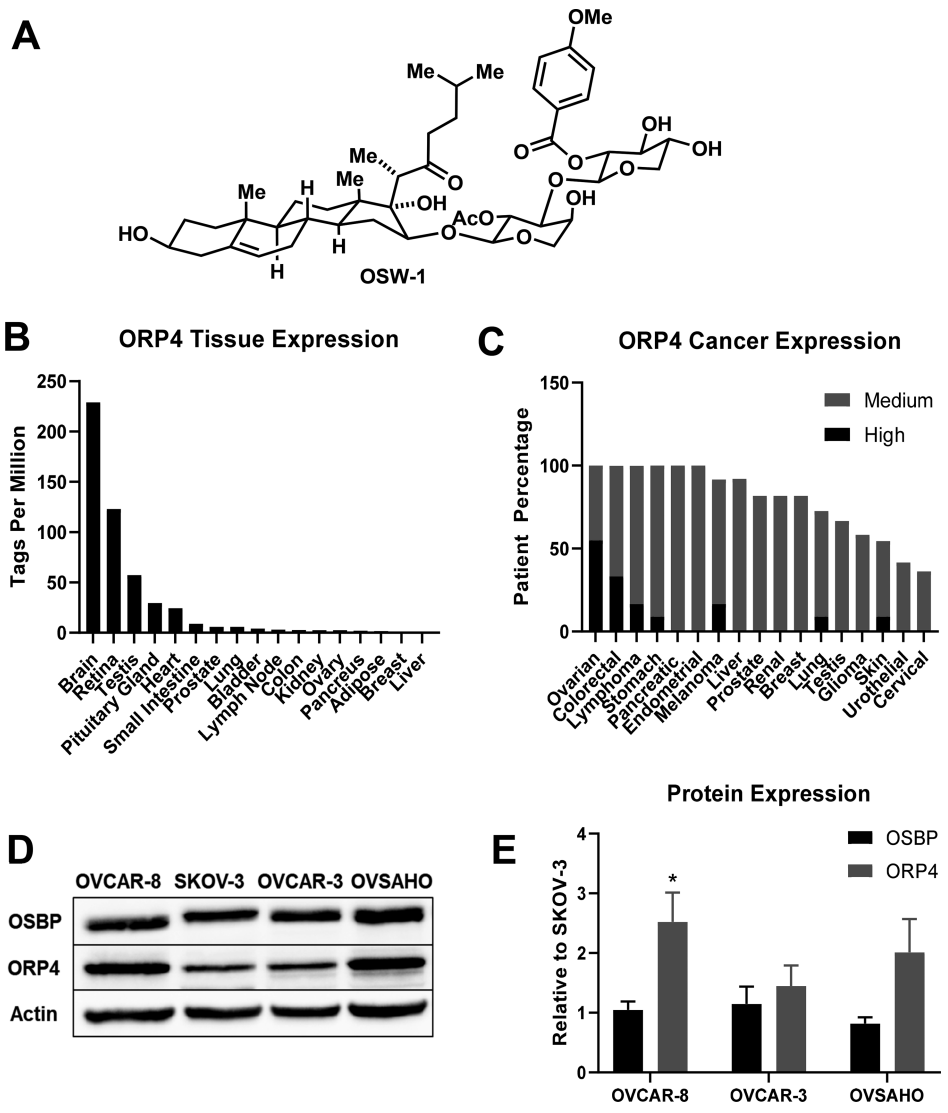

Figure 1. ORP4, a cellular target of the antiproliferative compound OSW-1, is selectively expressed in ovarian cancer cells. (A) The OSW-1 compound. (B) ORP4 RNA expression in human tissues from the FANTOM5 database.[42] (C) ORP4 expression in patient-isolated human cancer tissue; data were collected from the Human Protein Atlas. Patient samples ≥9. (D) Representative Western blot of OSBP and ORP4 expression in four ovarian cell lines: OVCAR-8, SKOV-3, OVCAR-3, and OVSAHO. (E) Western blot quantification of OSBP and ORP4 in ovarian cancer cell lines relative to SKOV-3. Average of three independent experiments..*p-value ≤0.05.

HGSC metastasis results in the dissemination of the cancer cells to vital organs throughout the peritoneal cavity, especially affecting the gastrointestinal and genitourinary systems.[3] The pathophysiology of HGSC causes ascites formation, which is correlated to increasing patient morbidity rates.[3,5] HGSC cells aggregate to form three-dimensional (3D) tumor spheroids in the ascites to avoid anoikis (i.e., programmed cell death caused by lack of cellular attachment) leading to the transcoelomic metastasis.[3,5] The multicellular structure of cancer spheroids in ascites depresses the efficacy of the SOC chemotherapy and promotes HGSC drug resistance.[3,5,6] In general, the ovarian cancer spheroids present in ascites are hypoxic and existing in a microenvironment with an atypical nutrient supply, including the supply of extracellular lipids.[7] Recent studies have indicated that the biosynthesis of cholesterol and other lipids are important in HGSC tumorigenesis and clinical response to chemotherapy.[8−11] Further, use of cholesterol-lowering statin drugs has been implicated on a population level in reducing ovarian cancer risk and in improving clinical outcomes in ovarian cancer patients.[12−16]

The clinical relevance of HGSC spheroids, especially in cancer therapeutic development studies, has led to the advancement of three-dimensional (3D) cell culturing methods in ovarian cancer.[17−21] *In vitro* ovarian cancer cell lines that form 3D spheroids model the *in vivo* HGSC spheroids, including mimicking transcriptome alterations and other HGSC spheroid characteristics.[19,20] *In vitro* 3D cell culture models are useful proxies of clinical cancer disease in ways that two-dimensional (2D) monolayer are not.[17,18,20] Due to this advantage, 3D cell culture models are used to identify and evaluate new anticancer agents *in vitro*.[18,22,23] Recently, we demonstrated that ovarian cancer 3D spheroids, regardless of size and shape, show similar drug resistance compared to the corresponding 2D monolayer cell lines.[21] Therefore, in this study, we investigated the effects of the novel anticancer compound OSW-1 in ovarian cancer cells cultured

https://dx.doi.org/10.1021/acsptsci.0c00207
ACS Pharmacol. Transl. Sci. 2021, 4, 744−756

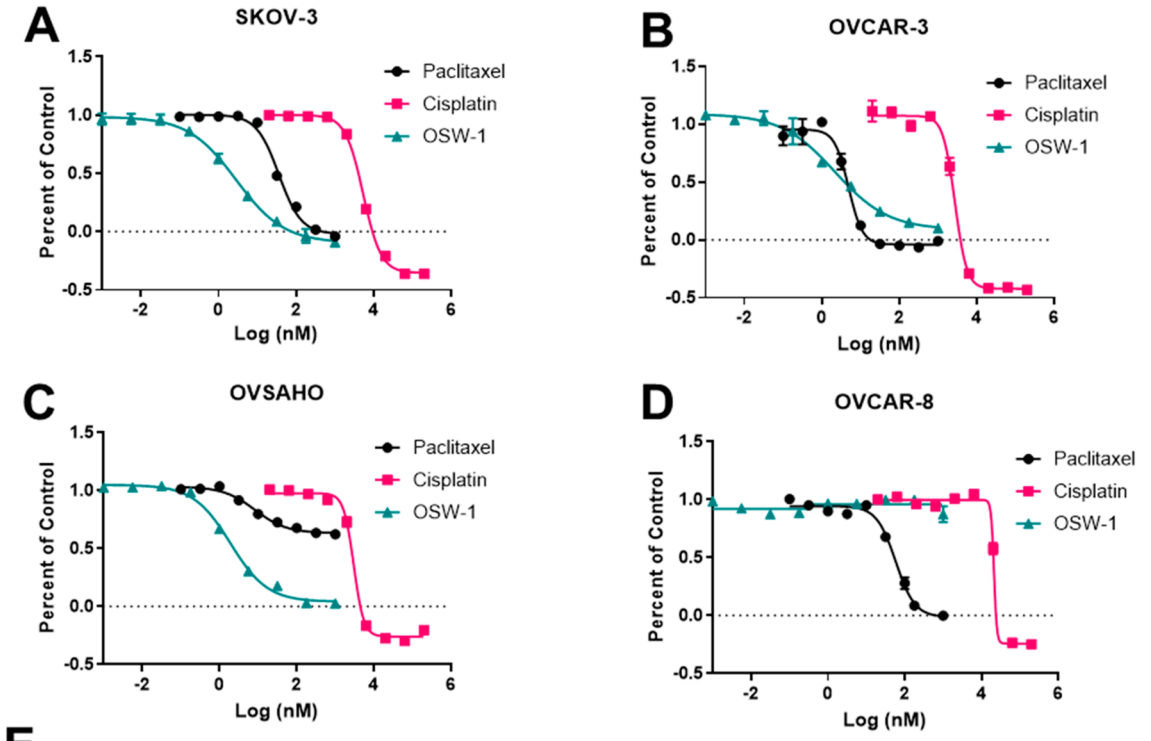

E

Cytotoxicity Against Ovarian Cancer Cell Lines (72 hour treatment)			
Monolayer Cell Culture (IC_{50} (nM))			
Cell Line	Paclitaxel	Cisplatin	OSW-1
SKOV-3	34 ± 3.2	7,800 ± 4,700	4.0 ± 2.7
OVCAR-3	6.9 ± 2.1	2,900 ± 360	2.2 ± 0.85
OVSAHO	N/Q (>1,000)	3,400 ± 1,200	1.8± 0.61
OVCAR-8	54 ± 8.4	22,000 ± 4,300	N/Q (>1,000)
Spheroid Cell Culture (concentration inducing a 50% reduction in cell population (nM))			
SKOV-3 spheroids	N/Q (>10,000)	N/Q (>10,000)	10
OVCAR-8 spheroids	1,000	10,000	100

Figure 2. OSW-1 is a cytotoxic agent to monolayer ovarian cancer cells following 72-h treatment. (A–D) Representative cell viability curves of paclitaxel, cisplatin, and OSW-1 in four ovarian cell lines after 72 h treatment. (E) Table of compound cytotoxicity values against ovarian cancer cell lines cultured as monolayer or spheroids. All values are averaged from three independent experiments. N/Q = not quantifiable, indicating the growth inhibition did not reach 50% at the maximum concentration tested.

in both 2D monolayer culture and the more clinically relevant 3D spheroids.

The natural product compound OSW-1 (Figure 1A), isolated from the bulbs of the *Ornithogalum saudersiae* plant, is an exceptionally potent cytotoxic agent against a wide range of *in vitro* cancer cell lines (NCI 60 Avg. IC_{50} = 0.78 nM).[24,25] OSW-1 induces its cellular effects through binding to oxysterol-binding protein (OSBP) and OSBP-related protein 4 (ORP4).[26−30] OSBP and ORP4 are cytoplasmic, non-enzymatic proteins belonging to a 12-member family of lipid transport and regulatory proteins.[31] OSBP and ORP4 bind oxysterols, including 25-hydroxycholesterol (25-OHC), with high affinity,[31] but OSBP and ORP4 are not involved in cholesterol biosynthesis.[31] OSBP is reported to be required for lipid transport between the endoplasmic reticulum (ER) and the Golgi.[32,33] OSBP transports cholesterol from the ER to the lysosome,[29] and OSBP is required for the replication of several classes of pathogenic ssRNA viruses.[27,28,34] However, OSBP does not have any known role in cellular viability, cellular proliferation, or cancer biology.[27,28,31] In contrast, ORP4 is an identified precision cancer target in certain leukemias and a driver of cancer cell proliferation.[30,35,36] Unlike the ubiquitous expression of OSBP, ORP4 is reported to have limited selective expression in normal tissue with only parts of the brain, retina, and testes showing significant ORP4 expression.[37] $ORP4^{-/-}$ mice develop normally, aside from male sterility, signifying the limited role of ORP4 in nontransformed tissue.[38] ORP4 is selectively expressed in patient-isolated T-cell acute lymphoblastic leukemia cells and drives the leukemia proliferation, including in leukemia stem cells.[30,35] ORP4 is also reported to promote mitochondrial respiration in immortalized immune cells by regulating calcium release from the endoplasmic reticulum through mediating a G-protein activation of PLC3β.[30,35] Knockdown of ORP4 in cancer cell lines results in increased apoptosis, autophagy, and mitochondrial dysfunction,[30,35,36,39,40] which phenocopies OSW-1 treatment.[41]

https://dx.doi.org/10.1021/acsptsci.0c00207
ACS Pharmacol. Transl. Sci. 2021, 4, 744−756

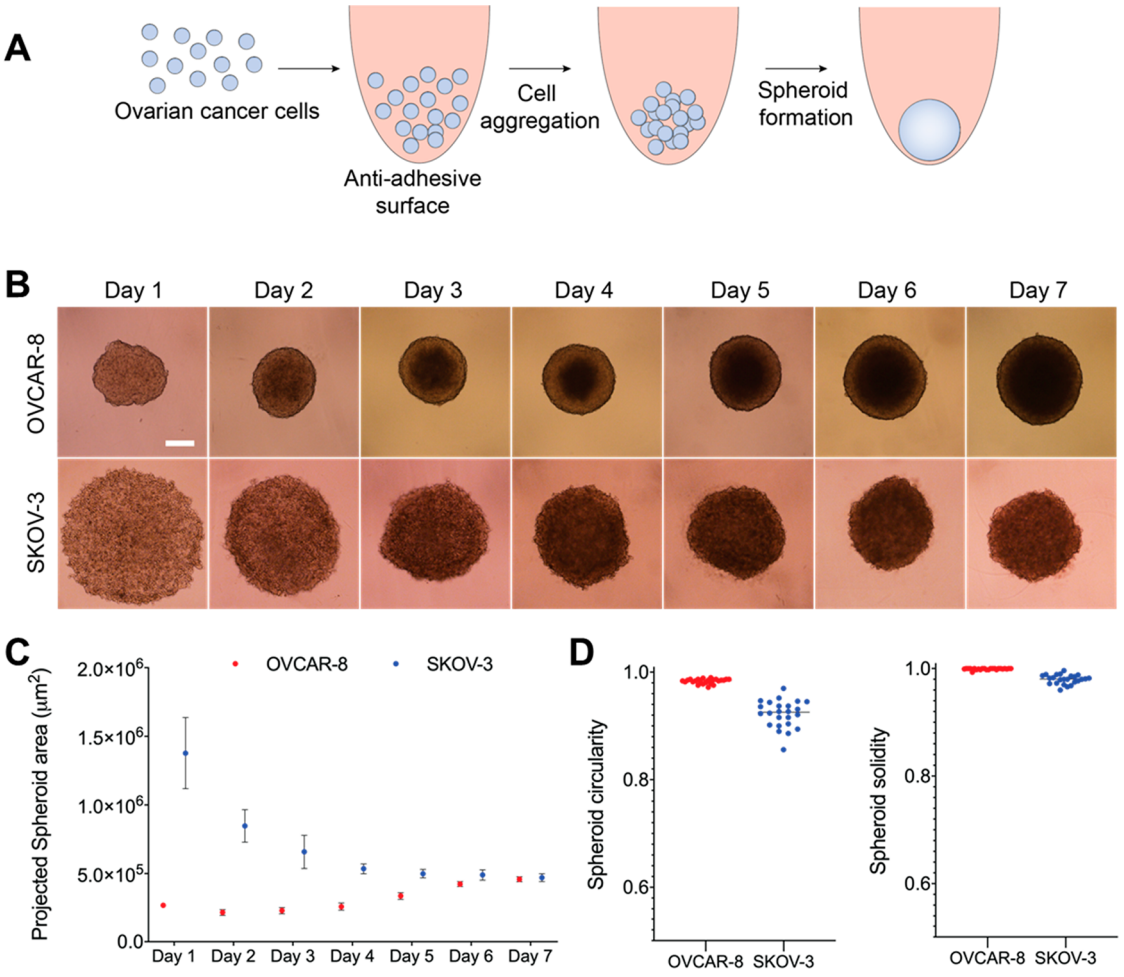

Figure 3. OVCAR-8 and SKOV-3 ovarian cancer cells form three-dimensional spheroids *in vitro*. (A) Schematic of spheroid formation in ovarian cell lines. (B) OVCAR-8 (10% FBS) and SKOV-3 (0% FBS) spheroid development over 7 days. White bar represents 250 μM. (C) Quantification of average spheroid area over 7 days using ImageJ software analysis. (D) Measurement of circularity and solidity of spheroid analysis at day 7 with ImageJ software analysis.

Previously, an OSW-1-derived compound, reported to selectively bind ORP4 over OSBP, showed anticancer efficacy and limited toxicity when administered daily for several weeks in a mouse leukemia model.[30]

Our recent work has demonstrated that a short-term, transient, and low dose (i.e., 1 nM for 6 h) treatment of OSW-1 induces a selective reduction of OSBP levels in multiple cancer cell lines.[27,28] This degradation persists for several days following removal of the compound with no signs of cellular toxicity or growth arrest.[27] These results suggests loss of OSBP function in cells does not induce cytotoxicity under normal cell culture conditions. Conversely, ORP4 expression is unchanged under these transient OSW-1 treatment conditions, but long-term OSW-1 treatment does induce a reduction of ORP4 levels (Figure 5).[27] These results suggest that the primary cause of cytotoxicity upon OSW-1 treatment is through affecting ORP4, not OSBP.[27]

According to the FANTOM database, ORP4 is highly expressed in human ovarian tumor samples (see Figure 1C[42]); however, according to our knowledge, there is no published study detailing the role of ORP4 in ovarian cancer. The OSW-1 compound is reported to be 40-fold more active against the SKOV-3 ovarian cancer cell compared to ovarian fibroblasts, and OSW-1 has low nanomolar cytotoxicity against the ovarian cancer cell lines present in the NCI-60 cancer cell line panel.[25,43] Herein, we describe the expression of ORP4 and the anticancer activity of the ORP4-targeting OSW-1 compound in a panel of ovarian cancer cell lines, including in ovarian cancer spheroids. We demonstrate that OSW-1 shows potent cytotoxicity, particularly relative to SOC chemotherapy agents cisplatin and paclitaxel, in both monolayer and spheroid ovarian cancer models. Using a simple and low-cost ultralow attachment technique, 3D spheroids of multiple ovarian cancer cell lines were produced and extensively characterized. We show that OSW-1 reduces ORP4 protein levels in both monolayer and spheroids models and that OSW-1 cytotoxicity occurs in the same time frame as the reduction of ORP4 levels. Lastly, we observed that the removal of extracellular lipids from the culture media, which could mimic the reliance of nonvascularized tumors on lipid biosynthesis,[8−11] significantly potentiated cytotoxicity of OSW-1. This amplified OSW-1 activity could be abrogated by the addition of free cholesterol to the culture media. Based on the reported role of OSBP in intracellular cholesterol transport, the potentiation of the OSW-1 compound activity under cholesterol-depleted conditions could be due to its interaction with OSBP and not ORP4. Overall, these results suggest that small molecule

https://dx.doi.org/10.1021/acsptsci.0c00207
ACS Pharmacol. Transl. Sci. 2021, 4, 744−756

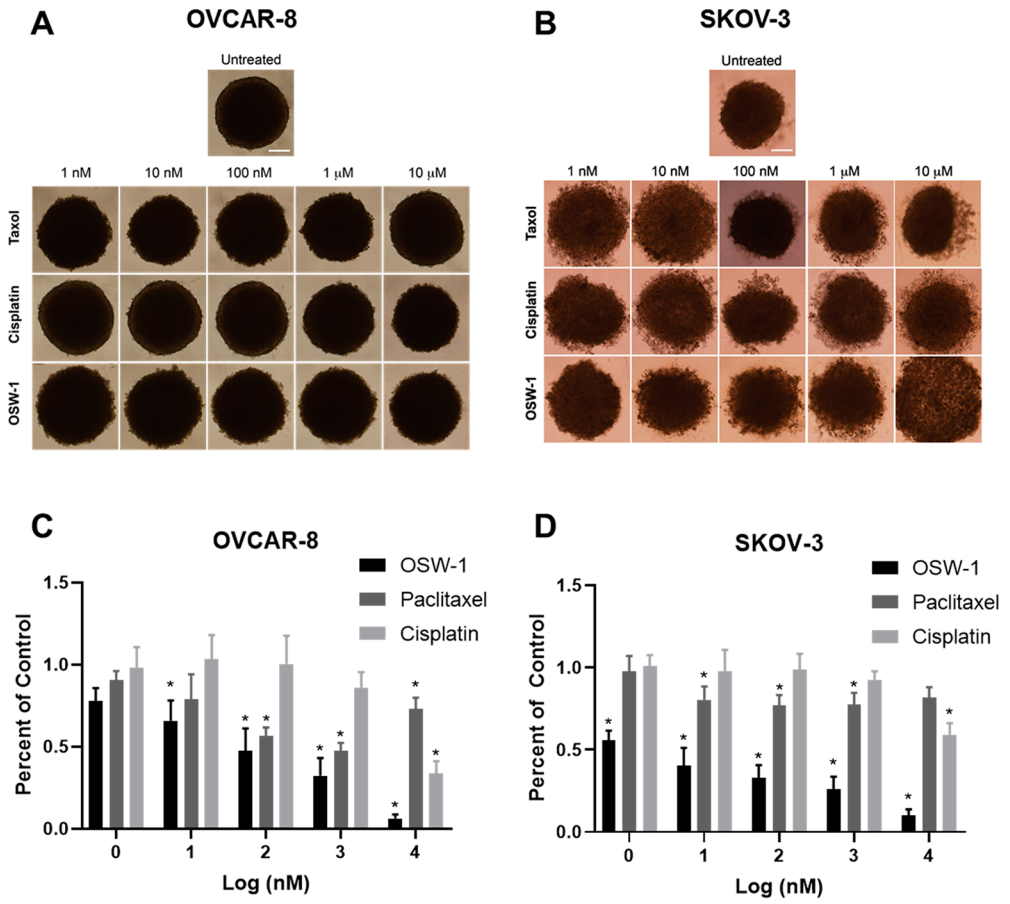

Figure 4. The OSW-1 compound is a potent, cytotoxic agent to *in vitro* generated ovarian cancer spheroids. (A) OVCAR-8 spheroids after 72 h post treatment with paclitaxel, cisplatin, or OSW-1. (B) SKOV-3 spheroid images after 72 h post treatment with paclitaxel, cisplatin, or OSW-1. (C) 72 h cytotoxicity measurements of OSW-1, paclitaxel, or cisplatin on OVCAR-8 spheroids, expressed as a percentage of DMSO vehicle control. Averaged results of three independent experiments. (D) 72 h cytotoxicity measurements of OSW-1, paclitaxel, or cisplatin on SKOV-3 spheroids, expressed as a percentage of DMSO vehicle control. Averaged results of three independent experiments. *p-value ≤0.05.

compounds targeting ORP4 and potentially OSBP represent a novel route for the potential treatment of ovarian cancer.

RESULTS

ORP4 is Ubiquitously Expressed in Ovarian Cancer Cells *in Vitro*. Analysis of the publicly available human RNA expression data sets from FANTOM[42] shows that ORP4 has minimal expression in healthy ovarian tissue but is highly expressed in ovarian cancers (Figure 1B, C). We confirmed ORP4 is highly expressed in the panel of four human HGSC immortalized cancer cell lines: SKOV-3, OVCAR-8, OVCAR-3, and OVSAHO. SKOV-3, OVCAR-3, and to a lesser extent OVCAR-8 are extensively used ovarian cell line model systems reported to be genetically dissimilar to patient-derived ovarian cancer samples.[44] Conversely, OVSAHO is reported to more closely recapitulate the biology of patient-isolated ovarian cancer samples.[44] All four ovarian cancer cell lines evaluated express ORP4 as measured by Western blot (Figure 1D). The OVCAR-8 and OVSAHO cell lines showed approximately twofold more ORP4 expression than SKOV-3 and OVCAR-3 (Figure 1D, E). In contrast, the level of relative OSBP expression did not significantly vary between the four cell lines (Figure 1D, E).

OSW-1 is a Potent Inhibitor of Ovarian Cancer Cell Proliferation. The cytotoxicity of OSW-1 (Figure 1A) was compared to chemotherapy SOC agents paclitaxel and cisplatin in the HGSC ovarian cancer cell line panel in a monolayer viability assay (Figure 2A–E). OSW-1 exhibited potent, low nanomolar cytotoxicity at 72 h against monolayers of three of the four ovarian cancer cell lines (SKOV-3, OVCAR-3, and OVSAHO), showing a higher potency than paclitaxel and cisplatin (Figure 2A–C). Unexpectedly, OSW-1 showed no effect on the OVCAR-8 monolayer cells at concentrations up to 1 μM (Figure 2B). Cisplatin and paclitaxel affected OVCAR-8 similarly to the other ovarian cancer cell lines (Figure 2A–E). Although not inducing cytotoxicity, OSW-1 did induce clear morphological changes in the OVCAR-8 cells in monolayer, including inducing cells with less cell-to-cell contact, at concentrations as low as 1.0 nM (Figure S-3A). Furthermore, the OVSAHO cell line showed resistance to paclitaxel (IC_{50} > 1 μM) but was still highly sensitive to OSW-1 (IC_{50} = 1.8 ± 0.61 nM). Together, these results suggest that OSW-1 is a potent, cytotoxic agent of ovarian cancer monolayer cells culture *in vitro* with the exception of the OVCAR-8 cell line.

***In Vitro* Spheroids Produced from Ovarian Cancer Cell Lines OVCAR-8 and SKOV-3 Using a Low Attachment Method.** 3D tumor spheroids are reported to provide a better representation of *in vivo* tumors compared to conventional 2D culture.[18,22,23] We prepared OVCAR-8 and SKOV-3 spheroids using methods we previously developed and validated (Figure 3A).[21] The OVSAHO and OVCAR-3 cell

https://dx.doi.org/10.1021/acsptsci.0c00207
ACS Pharmacol. Transl. Sci. 2021, 4, 744–756

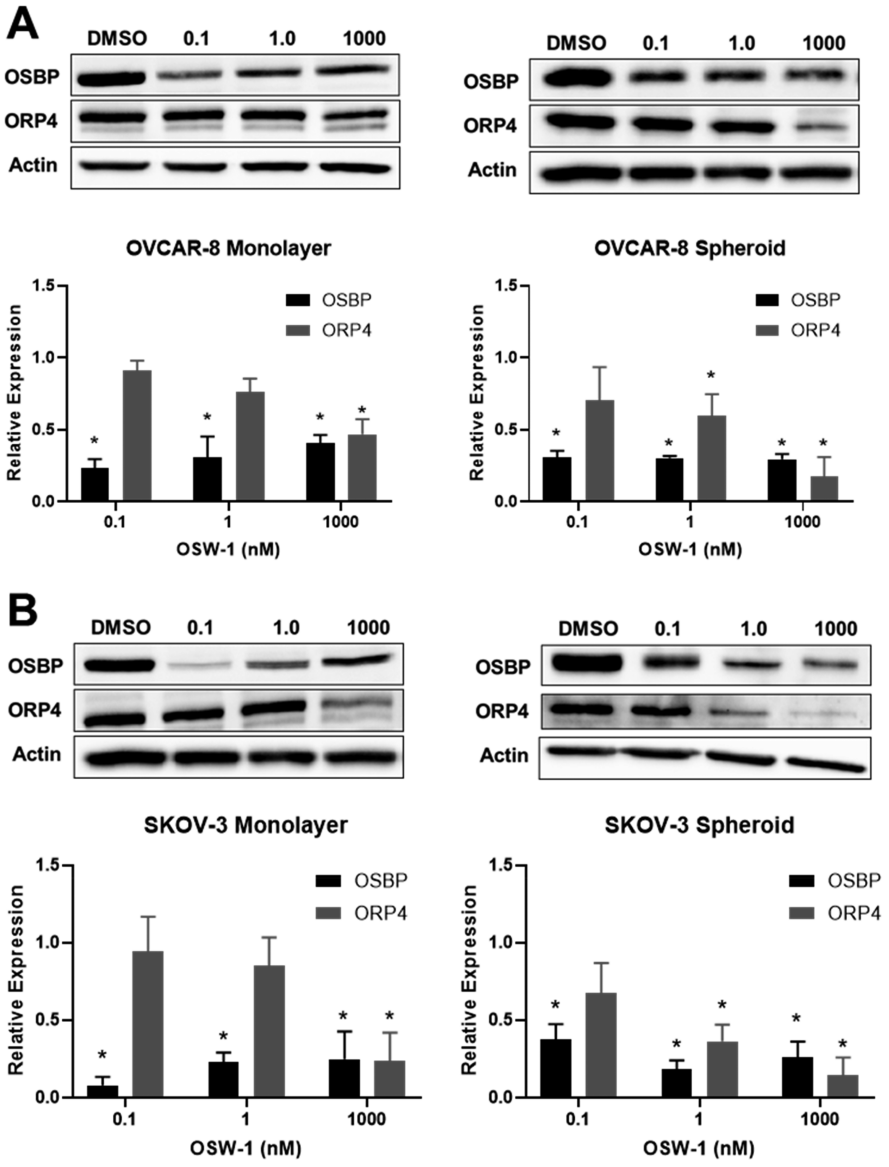

Figure 5. Ovarian cancer viability decreases with loss of ORP4 expression, but not OSBP expression, upon OSW-1 treatment. (A) OSBP and ORP4 protein expression in monolayer and spheroids following the provided treatments of OSW-1 for 48 h in OVCAR-8. Representative Western blot and average of three independent experiments shown. (B) OSBP and ORP4 protein expression in monolayer and spheroids following the provided treatments of OSW-1 for 48 h in SKOV-3. Representative Western blot and average of three independent experiments shown. *p-value $\leq$0.05.

lines did not form compact spheroids and were not used in this study (data not shown). An optimization study (Figure S-1) determined that 5000 OVCAR-8 cells and 20 000 SKOV-3 cells produced spheroids with similar surface area measurements after 7 days of incubation (Figure 3C). The OVCAR-8 cells aggregated within the first 24 h and had clear spheroid boundaries at 48 h (Figure 3B). The OVCAR-8 spheroids continued to expand in size throughout the 7-day incubation (Figure 3B). The presence of FBS in the media disrupted SKOV-3 spheroid formation around day 4 (Figure S-4). Based on reports of serum-free spheroid formation,[45,46] SKOV-3 spheroids were cultured in FBS-free media, producing spheroids with clear boundaries after 4 days (Figure 3B). Circularity and solidity measurements were carried out on day 7 (Figure 3C). Both the OVCAR-8 and SKOV-3 spheroids at day 7 had a circularity measurement of >0.9 (Figure 3D) and solidity measurement of >0.95 (Figure 3D), indicating the formation of mature, dense, and circular spheroids.[47] As a result, we performed all cytotoxicity measurements on 7-day-old spheroids.

OSW-1 is a Potent Cytotoxic Agent in *in Vitro* Ovarian Cancer Spheroids. Seven-day-old OVCAR-8 and SKOV-3 spheroids were treated for 72 h with paclitaxel, cisplatin, or OSW-1 in complete, FBS-containing media (Figure 4A–D, Figure 1E) and assayed for cytotoxicity. As mentioned previously, 5000 OVCAR-8 cells and 20 000 SKOV-3 cells were initially used to produce the same-sized spheroids on day 7. Paclitaxel reduced ~50% of the viable cell population at 100 nM in OVCAR-8 spheroids (Figure 4A, C), as compared to a paclitaxel IC_{50} value of 6.9 ± 2.1 nM in OVCAR-8 monolayer (Figure 2D, E). Cisplatin showed approximately the same micromolar cytotoxicity potency in the OVCAR-8 monolayer (Figure 2D, E) as in the spheroids (Figure 4A, C). OSW-1 was more cytotoxic in the OVCAR-8 spheroids (<50% cell

https://dx.doi.org/10.1021/acsptsci.0c00207
ACS Pharmacol. Transl. Sci. 2021, 4, 744–756

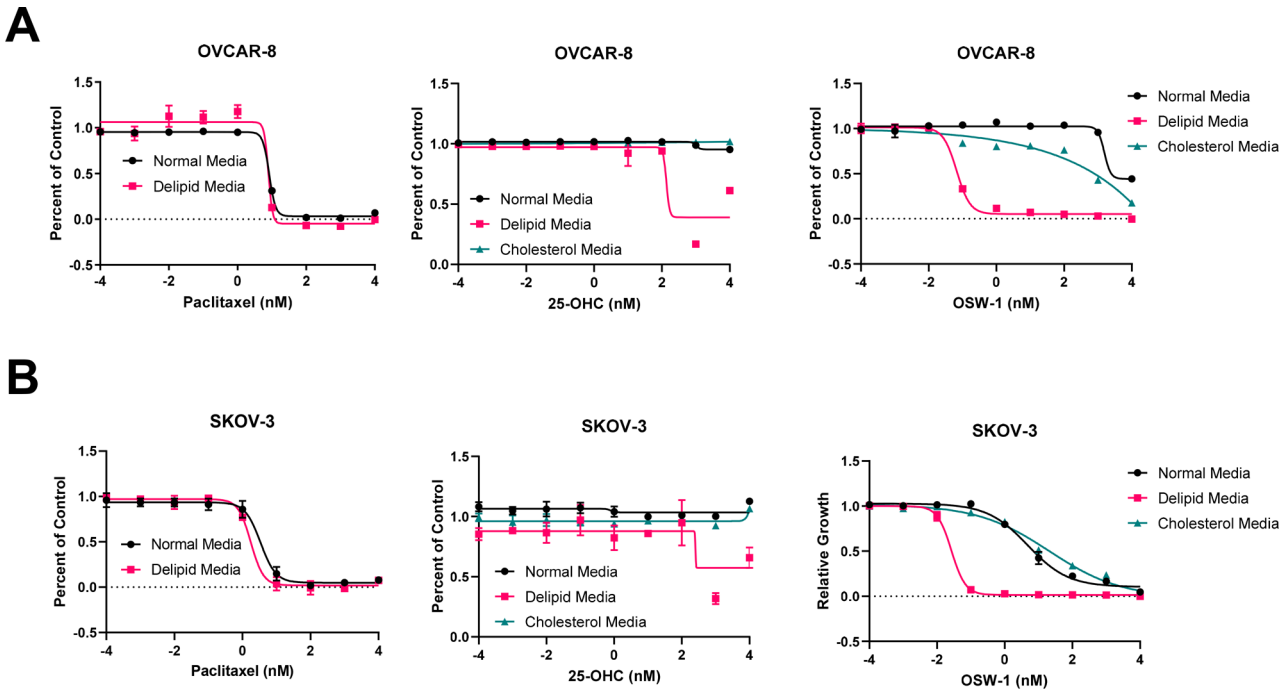

C

IC_{50} Fold Change Relative to Normal Media				
	OVCAR-8		SKOV-3	
	Delipid	Cholesterol	Delipid	Cholesterol
Paclitaxel	-3.7	N/A	-2.0	N/A
25-OHC	> -84	N/Q	> -62	N/Q
OSW-1	-1.7×10^5	N/Q	-180	2.1

Figure 6. OSW-1 cytotoxicity is potentiated by the absence of extracellular cholesterol. (A) Cell viability curves of 2D OVCAR-8 cells grown in either normal media (RPMI with 10% FBS), delipidated media (RPMI with 10% delipidated FBS), or cholesterol-supplemented delipidated media (RPMI with 10% delipidated FBS and 20 μg/mL cholesterol), treated with paclitaxel, 25-OHC, or OSW-1 for 72 h. (B) Cell viability curves of 2D SKOV-3 cells grown in either normal media (RPMI with 10% FBS), delipidated media (RPMI with 10% delipidated FBS), or cholesterol-supplemented delipidated media (RPMI with 10% delipidated FBS and 20 μg/mL cholesterol), treated with paclitaxel, 25-OHC, or OSW-1 for 72 h. (C) Fold change compared to cell cultured with normal media (RPMI with 10% FBS) compared to cells treated with paclitaxel, 25-OHC, or OSW-1 in either delipidated media (i.e., Deplid) or exogenously added cholesterol (i.e., Cholesterol). IC_{50} values used to calculate the fold change are the average of three independent experiments. N/Q = not quantifiable due to curves failing to conform to dose−response curve shape. N/A = not attempted.

numbers at 100 nM) than in the monolayer (IC_{50}> 1 μM.) The SKOV-3 spheroids were more resistant to paclitaxel and cisplatin compared to the OVCAR-8 spheroids. Paclitaxel and cisplatin treatment of up to 10 μM failed to reduce the SKOV-3 spheroid cell numbers by 50% (Figure 4D, Figure 1E). In contrast, OSW-1 showed high potency against the SKOV-3 spheroid viability (Figure 4B, D); approximate cell population was reduced ∼50% at 1 nM, which is comparable to the OSW-1 cytotoxicity in monolayer SKOV-3 model (IC_{50} = 4.0 ± 2.7 nM) (Figure 2A, E). Confirming the potency of OSW-1 against the SKOV-3 spheroids, 100 nM OSW-1 treatment for 48 h disrupted the boundary morphology of the SKOV-3 spheroids, but paclitaxel and cisplatin treatments up to 10 μM had minimal effects on spheroid boundary morphologies (Figure S-2). These results indicate that OSW-1 is a more potent cytotoxic agent against 3D ovarian cancer cell line spheroid models compared to SOC agents paclitaxel and cisplatin.

OSW-1 Cytotoxicity Is Related to ORP4 Levels in Monolayer and Spheroids. Our previous studies have demonstrated that low-dose OSW-1 treatment (i.e., 1 nM) results in the selective reduction of OSBP protein levels by more than 90% in monolayer cancer cell models, while treatment with paclitaxel or other cytotoxic compounds did not affect OSBP levels.[27,28] We also reported that OSW-1 treatment partially reduces ORP4 levels in cancer cells, but the ORP4 reduction requires longer and higher concentration treatments of OSW-1 compared to treatments capable of reducing OSBP levels.[27,28] Based on these previous results, the effects of OSW-1 treatment on OSBP and ORP4 levels were analyzed upon OSW-1 treatments in monolayer and spheroid ovarian cancer cells (Figure 5). OSW-1 begins to induce cytotoxicity between 24 and 48 h in SKOV-3 and OVCAR-8 monolayer cell cultures (Figures S-3A and S-3B); after 72 h OSW-1 treatment, cell death was evident. Therefore, the effects of OSW-1 on OSBP and ORP4 levels were determined after 48 h of OSW-1 treatment to avoid nonviable cells in the analysis.

Forty-eight hour OSW-1 treatments at 0.1 nM, 1 nM, and 1 μM all reduced OSBP levels approximately to the same level

https://dx.doi.org/10.1021/acsptsci.0c00207
ACS Pharmacol. Transl. Sci. 2021, 4, 744−756

(i.e., >60% reduced) in both SKOV-3 and OVCAR-8 monolayer and spheroid cultures (Figure 5A, B, Figure S-3B). The similar reduction in OSBP levels in both the monolayer and the spheroids indicates OSW-1 is able to penetrate into the spheroids, affecting the overall spheroid cell population. As shown (Figure 2A, D, E), SKOV-3 cells are much more sensitive to OSW-1 than the OVCAR-8 cells. Considering the dramatic difference in OSW-1 cytotoxicity in SKOV-3 and OVCAR-8 cells, the uniform reduction of OSBP upon OSW-1 treatment in both cell lines suggests OSBP reduction is independent of cytotoxicity.

ORP4 protein levels are also reduced after 48 h OSW-1 treatment in both monolayer and spheroids in both OVCAR-8 and SKOV-3 cell lines. The timing of the OSW-1-induced reduction of ORP4 levels coincides with the OSW-1-induced cytotoxicity in SKOV-3 and OVCAR-8 cells in monolayer culture (Figure 5, Figure S-3): SKOV-3 cells, which are sensitive to OSW-1 in monolayer (IC_{50} = 4.0 ± 2.7 nM) (Figure 2A, E), showed more pronounced reduction of ORP4 than the OSW-1-refractory OVCAR-8 monolayer culture (IC_{50} > 1.0 μM) (Figure 2D, E). OSW-1 treatment also causes reduction of ORP4 (i.e., >80% reduction at 1 μM of OSW-1 treatment) in both the SKOV-3 and OVCAR-8 spheroids (Figure 5). OSW-1 treatment causes more reduction of ORP4 in the OVCAR-8 spheroids than the OVCAR-8 monolayer cells (Figure 5), which matches the higher cytotoxicity of OSW-1 in the OVCAR-8 spheroids than the OVCAR-8 monolayer culture (Figures 2 and 4).

Extracellular Lipids and Free Cholesterol Levels Alter OSW-1 Cytotoxicity in Monolayer Ovarian Cancer Cells. Cholesterol homeostasis has recently been shown to affect ovarian cancer cell sensitivity to anticancer drugs.[48] To model the activity of OSW-1 under lipid deficient conditions, monolayer OVCAR-8 and SKOV-3 cells were cultured in delipidated media.[49] The lipid-depleted OVCAR-8 and SKOV-3 cells showed no significant changes in growth or morphology (Figure S-5). However, the ovarian cancer cells cultured in lipid-depleted media showed far more cytotoxicity to OSW-1 after 72 h (Figure 6A−C). OVCAR-8 cells exhibited a >170 000-fold increased cytotoxicity to OSW-1 after 72 h under lipid-depleted growth conditions (IC_{50} = 0.06 ± 0.02 nM) (Figure 6A, C). This effect was also seen in SKOV-3 with a ∼180-fold increase in OSW-1 cytotoxicity after 72 h in lipid-depleted media (IC_{50} = 0.02 ± 0.01 nM) (Figure 6B, C). 25-Hydroxycholesterol (25-OHC) is a high affinity ligand for both OSBP and ORP4.[26,27] In contrast to OSW-1, 25-OHC is weakly cytotoxic with IC_{50} values of >10 mM.[26] Also, 25-OHC does not induce the reduction of OSBP levels in cells.[26] Further, unlike OSW-1, 25-OHC has several cellular effects independent of OSBP and ORP4, including inhibiting cholesterol biosynthesis through binding to INSIG.[50] Lipid-depleted culture conditions also increased the cytotoxicity of 25-OHC in SKOV-3 and OVCAR-8 cells to a nanomolar range (IC_{50} = 160 ± 77 nM, IC_{50} = 120 ± 10 nM, respectively) (Figure 6A−C). Paclitaxel cytotoxicity was not significantly changed due to delipidated growth conditions (p-value >0.05) (Figure 6A−C).

Importantly, the addition of 20 μg/mL free cholesterol to the lipid-depleted media reversed the significant increase in potency of OSW-1 in the lipid-depleted media in both the SKOV-3 and OVCAR-8 cells, resulting in no significant difference compared to normal media (p-value >0.05) (Figure 6A−C). Also, the addition of exogenous cholesterol completely reversed the 25-OHC-induced cytotoxicity present under delipidated conditions (Figure 6A−C). These results suggest that ovarian cancer cells under growth condition deprived of exogenous cholesterol are highly sensitive to small molecule targeting of OSBP and ORP4.

DISCUSSION

The discovery that the anticancer small molecule OSW-1 targets OSBP and ORP4 presents a potentially novel antiproliferative mechanism of action for precision cancer therapeutic development.[26,30,35,36] ORP4 is reported to be essential for cancer cell viability and proliferation, whereas OSBP is not reported to be involved in cell viability or proliferation.[26,27,30,35,36] In this study, we showed that OSW-1 is a potent inhibitor of ovarian cancer cell proliferation *in vitro* in both monolayer (Figure 2) and spheroids (Figure 4). With the exception of the OVCAR-8 monolayer culture, the OSW-1 compound is more active in inhibiting ovarian cancer proliferation than either of the SOC agents paclitaxel or cisplatin (Figure 2, **4**) particularly in the spheroid cytotoxicity assay (Figure 4). The *in vivo* HGSC spheroids that form in clinical ovarian cancer cases frequently acquire resistance to SOC chemotherapy, and the nonvascularized HGSC spheroids likely prevent drug penetrance and therapeutic efficacy.[18] The relative inefficacy of paclitaxel and to a lesser extent cisplatin in the *in vitro* 3D ovarian cancer spheroid model (Figure 4) is consistent with published results.[21,51]

We showed that the OSW-1 treatment reduces cellular OSBP and ORP4 in the ovarian cancer cells culture in both the monolayer and spheroid models, and the OSW-1 cytotoxicity is correlated with the reduction of the ORP4 protein and was independent of OSBP reduction (Figure 5) in both *in vitro* models. The capability of the OSW-1 compound to reduce OSBP and ORP4 levels (Figure 5) and inhibit the growth by 90% in spheroids of OVCAR-8 and SKOV-3 (Figure 4) suggests widespread penetration of the compound in the spheroids. OSW-1 caused a marked reduction in OSBP levels (i.e., >60% reduction) in both SKOV-3 and OVCAR-8 cell lines in both monolayer and spheroid cultures at concentrations as low as 100 pM treatment (Figure 5) after 48 h. Previously, in nonovarian cancer cell lines, OSW-1 treatment is reported to reduce OSBP levels after 4 h of treatment; reduction of ORP4 levels required much longer exposure of 12−24 h.[27] These results suggest that ORP4 is the anticancer target of OSW-1, and the high levels of ovarian-cancer-specific expression of ORP4 (Figure 1B−E) indicates it as a potential target in ovarian cancer.

Alternatively, OSW-1 could also be altering the function of OSBP and ORP4 prior to triggering the cellular processes leading to their reduction. The functional disruption of OSBP and ORP4 levels could lead to the antiproliferative response instead of the reduction in protein levels. Recent reports suggest that ORP4 is an important scaffolding protein in leukemia cells that complexes several proteins to activate PLCβ3.[30,35,52] If ORP4 executes the same or similar role in ovarian cancer, the decrease in its cellular levels caused by OSW-1 treatment is likely to be required for the anticancer activity, as opposed to OSW-1 inhibiting ORP4 function.

Due to poor vascularization, HGSC tumors and many other cancer tumors are believed to rely on cholesterol provided via biosynthesis.[8−11] Statin drugs, as inhibitors of cholesterol biosynthesis, are being studied as providing an effect in treating and preventing ovarian cancer.[8−11] Ovarian cancer cells

https://dx.doi.org/10.1021/acsptsci.0c00207
ACS Pharmacol. Transl. Sci. 2021, 4, 744−756

cultured under lipid-depleted conditions could recapitulate a lack of exogenous cholesterol experienced in the *in vivo* tumor microenvironment, which promotes tumor reliance on cholesterol biosynthesis.[8,53,54] Therefore, the strikingly enhanced potency (i.e., ~170 000 fold increase in cytotoxicity in OVCAR-8 cells) (Figure 6) of OSW-1 under lipid-depleted conditions indicates that the compound would be more effective under cholesterol-starved biological conditions (Figure 6), which may be a characteristic of HGSC tumors *in vivo*.[8,10] The reversal of the enhanced OSW-1 activity through the addition of free cholesterol to the lipid-depleted culture media (Figure 6) indicates cholesterol, and not another lipid, is responsible for the enhancement of OSW-1 potency. The enhanced potency to anticancer drugs under lipid-depleted conditions is specific to OSW-1; the cytotoxicity of paclitaxel, for example, is not affected by lipid-depleted media (Figure 6).

However, OSBP, not ORP4, is likely responsible for the striking shift in sensitivity to OSW-1 under lipid-depleted growth conditions. OSBP is not involved in cholesterol biosynthesis, but has an important role in cellular cholesterol sensing.[31] A recent paper shows that OSBP regulates mTORC1 activity by transferring cholesterol from the ER to the lysosomal membrane.[29] OSW-1 treatment was shown to block this OSBP cholesterol trafficking activity, thereby inhibiting mTORC1 activity, while ORP4 is not involved in direct mTORC1 regulation.[29] Our previous work showed that the degradation of the OSBP protein caused by OSW-1 did not cause cytotoxicity or effect proliferation in the presence of extracellular lipids.[27,28] Hypothetically, tumor cells reliant on cholesterol biosynthesis could be sensitive to interruptions of intracellular cholesterol trafficking executed by OSBP.[8−11] Cancer cells that are in the core of the tumor or spheroid could be especially sensitive to OSBP inhibition or reduction.

Significantly, a report showed that OVCAR-8 cells were much more sensitive than SKOV-3 cells to a combined statin and 25-OHC treatment.[55] 25-OHC was used in this report to inhibit SREBP-2-induced upregulation of cholesterol biosynthesis, but 25-OHC does have pleiotropic cellular effects through interacting with several proteins, including OSBP.[31] The sensitivity of OVCAR-8 cells to the combination statin/25-OHC treatment was attributed to reduced cholesterol and geranylgeranyl levels in the cells, with the hypothesis that OVCAR-8 cells have a greater deficiency in either cholesterol biosynthesis or exogenous cholesterol update compared to the SKOV-3 cells.[55] The relative sensitivity of the OVCAR-8 spheroids to OSW-1 compared to the OVCAR-8 monolayer cells (Figures 2 and 4) would be consistent with OVCAR-8 cells having a vulnerability in supplying cholesterol, which is exasperated in the 3D spheroid. However, our results also suggest that OSBP inhibition, either with 25-OHC or OSW-1, could interfere with cholesterol transport in cells rather than total cholesterol levels, and that OVCAR-8 vulnerability to cholesterol-limited growth conditions could be due to a potential defect in intracellular cholesterol transport, leading to cholesterol deficiencies at specific locations in the cell. If this hypothesis is correct, OVCAR-8 under cholesterol-starved conditions, such as in spheroids, would become highly dependent on OSBP intracellular cholesterol transport and therefore highly sensitive to OSW-1 activity. OVCAR-8 cells grown in monolayer culture with excess cholesterol available might have little reliance on OSBP intracellular transport function due to cell line abnormalities in cholesterol uptake, biosynthesis, or distribution. This lack of reliance on OSBP, combined with the high ORP4 expression levels (Figure 1D, E) would explain the resistance of OVCAR-8 to OSW-1 treatment in monolayer, the higher sensitivity to OSW-1 in OVCAR-8 spheroids, and the extreme shifts in OSW-1 sensitivity under lipid depletion growth conditions.

If this hypothesis is correct, the OSW-1 compound would potentially have two modes of precision anticancer activity in ovarian cancer: (1) blocking the required proliferative activity of ORP4, which is selectively expressed in the ovarian cancer cells (Figure 1), and (2) selectively inhibiting OSBP in the tumor cells, which exist with little to no exogenous cholesterol being supplied due to a lack of vascularization. More mechanistic research is required for understanding the exact mechanism of OSBP in cancer.

Recent published work showed that daily administration of significant amounts of OSW-1 in an animal model showed only moderate toxicity after several weeks, and that an OSW-1 analog compound purported to be specific for ORP4 was efficacious with little toxicity in a mouse leukemia model.[30] These results suggest that OSW-1-derived compounds can be developed to specifically target OSBP or ORP4 and potentially advanced for anticancer drug development. Our work indicates that ovarian cancer will be a suitable cancer to explore ORP4 and OSBP targeting compounds, through developing OSW-1-derived compounds or other classes of compounds.

In conclusion, we showed OSW-1 showed orders of magnitude higher toxicity in spheroids cultures of ovarian cancer models compared to the SOC compounds paclitaxel and cisplatin. The cytotoxicity of OSW-1 does coincide with the reduction of the ORP4 expression but not the reduction of OSBP expression, suggesting loss of ORP4 is the major route of OSW-1 antiproliferative activity. In the absence of extracellular lipids, OSW-1 has enhanced cytotoxicity, which can be reversed through addition of free cholesterol to the culture media. However, this increased potency of OSW-1 is suggested to be independent of cholesterol biosynthesis inhibition, as demonstrated by the treatment of 25-OHC, and may be caused by the OSW-1 compound affecting OSBP and not ORP4. Further research will be required to delineate the roles and therapeutic potential of ORP4 and OSBP in ovarian cancer, including through the development of selective compounds capable of targeting only OSBP or ORP4.

MATERIALS AND METHODS

Cell Culture. Authentication of all cell lines using STR profiling was completed by University of Arizona Genetics Core immediately before use in the experiments. Cell lines were also confirmed to be mycoplasma-free. OVCAR-3 (ATTC #HTB-161), OVCAR-8 (NCI-Vial Designation 0507715), and OVSAHO (JCRB-1046) were cultured with RPMI Medium (Thermo 22400105) with the addition of 10% Hyclone (Fisher Sci SH3006603) and 1% penicillin−streptomycin (Thermo 15140122). SKOV-3 (HTB-77) were cultured in McCoy 5A media (Thermo 16600108) supplemented with 10% Hyclone and 1% penicillin−streptomycin. All mammalian cell lines were cultured at 37 °C in 5% CO_2 in either Nunclon Delta 10 cm^2 dishes (VWR 10171744), T25 flask (CellStar 690160), or T75 flask (TPP 90076).

2D Viability Assay. 5.0×10^3 cells/well were seeded in a 96-well plate with 75 μL media. Compounds (paclitaxel, cisplatin, or OSW-1) were serial diluted at 4× concentration in media. Twenty-five microliters of compound containing media

https://dx.doi.org/10.1021/acsptsci.0c00207
ACS Pharmacol. Transl. Sci. 2021, 4, 744−756

was added to 75 μL of cells, resulting in a 1× dilution of drug. Following a 72 h incubation, CellTiter-Blue was added for 20 h, and fluorescence was measured (544 nm excitation; 590 nm emission) using a GloMax Discover Microplate Reader. Cell culture growth relative to untreated cells were calculated expressed as IC_{50} values on Graphpad Prism software utilizing the four-parameter dose−response curve.

Spheroid Development. Spheroid formation was induced by the ultralow attachment technique in 96-well plates. Briefly, round-bottom 96-well plates (CELLTREAT 229590) were treated with antiadherence rinsing solution (STEMCELL 07010) by centrifuging the plates at 1300*g* for 5 min. The solution was aspirated, and wells were washed with basal media. OVCAR-8 spheroids were cultured in complete FBS-containing media. SKOV-3 spheroids cells were cultured in FBS-free media; SKOV-3 spheroids incompletely formed in FBS containing media (see Figure S-4). OVCAR-8 or SKOV-3 cells were seeded in 200 μL of media at the desired cell number, and plates were centrifuged at 100*g* for 3 min. For OVCAR-8 spheroids, every 24 h, 100 μL of culture media was removed, and 100 μL of fresh media was added. For SKOV-3 spheroids, the initial media was not changed until day 4. Starting on day 4, 100 μL of media was removed, and 100 μL of fresh media was added every 24 h. Spheroid formation was observed for 7 days by monitoring the formation every 24 h with bright field imaging. Spheroids were characterized for their surface area, circularity, and solidity by using ImageJ accordingly with the following formulas, as done previously.[47]

$$\text{circularity} = \frac{(4\pi \times \text{area})}{\text{perimeter}^2}$$

$$\text{solidity} = \frac{\text{area}}{\text{convex area}}$$

Spheroid Compound Treatment and Cell Viability Assay. Spheroids were treated with either 0.1% DMSO (for solubility) or compound-containing complete media in complete FBS-containing media for the indicated times. 3D spheroid viability was measured by using CellTiter-Glo3D.[56,57] Briefly, room temperature 100 μL of CellTiter-Glo3D solution was added to 100 μL spheroid solution. Contents were vigorously mixed to induce lysis of the spheroid and efficient extraction of ATP. Plates were incubated at room temperature for 25 min for stabilization of luminescent signal, followed by luminescence measurements with an integration time of 1 s per well on a GloMax Discover Microplate Reader according to the manufacturer's instructions. Cytotoxicity was calculated relative to an untreated control group. No spheroids were cultured on the outside wells of the 96 well plate to avoid edge effect.

Cell Lysis. To detach adherent cells, the media was aspirated, the cells were washed with 1× PBS, and TrypLE Express (Gibco 12605-010) was added to cells, followed by a 10 min, 37 °C incubation. Complete media was then added to neutralize the trypsin, and cells were spun at 14 000 RCF for 0.45 min at 4 °C. Then, supernatant was aspirated, and the cell pellet was washed with 1× PBS, followed by resuspension in 50 μL of AC lysis buffer. AC lysis buffer[27] consists of 150 mM NaCl, 1.5 mM $MgCl_2$, 5% glycerol, 0.8% NP40, 1 mM DTT, 50 mM HEPES, 25 mM NaF, and 1 mM Na_3PO_4) with 3× HALT/EDTA protease inhibitor (Thermo 78438) and 0.2 mM phenylmethanesulfonylfluoride (Goldbio). Cells were freeze/thawed (3×) with liquid nitrogen and centrifuged for 15 min at 14 000 RCF at 4 °C. The protein concentration of the resulting cellular lysate was determined with a Bradford assay.

Immunoblotting. SDS-PAGE gels (8.5%) were loaded with 25 μg of protein and transferred to a nitrocellulose membrane (Bio-Rad 1620115) with a constant voltage of 100 V for 1 h at 4 °C. The membrane was blocked in 5% milk for 0.5 h. Following washing with TBST (3×), the membrane was incubated with 1:500 ORP4 antibody (Santa Cruz sc-365922) or 1:1000 OSBP antibody (Santa Cruz sc-365771) overnight at 4 °C. Following washing, the membrane was incubated with 1:3000 secondary antibody (Santa Cruz sc-2060) for 1 h at RT. Following washing, the membrane was developed with ClarityTM Western ECL substrate (Bio-Rad 1705061) and imaged on the Bio-Rad ChemiDocTM Touch Imaging System. The membrane was incubated with 1:1000 β-actin HRP (Santa Cruz sc-47778 HRP) after washing and developed as previously described.

Trypan Blue Viability. Following compound treatment, the culture media was removed from the flask and kept. The adherent ovarian cancer cells were washed with 1× PBS, and then 2.5 mL TrypLE Express was added. Cells were incubated for ∼10 min at 37 °C to fully detach the cells, and then recovered complete compound media was added to inactivate the trypsin. The total cell count and cell viability count was performed using Trypan Blue staining (Thermo 15250061) with a TC20 automated cell counter (BioRad).

Preparation of Lipid-Depleted Fetal Bovine Serum. FBS was lipid-depleted following the Brown and Goldstein modification of the method developed by Cham and Knowles.[49] Briefly, 50 mL of FBS was added to a mixture of *n*-butanol and diisopropyl ether in a 40:60 (v:v) ratio. The solution was incubated for 20 min at RT followed by a 20 min of incubation on ice. The solution was centrifuged at 2000 rpm for 2 min. The lower aqueous fraction was isolated and re-extracted with 50 mL of diisopropyl ether followed by centrifugation. The resulting aqueous phase was evaporated to a volume of 20 mL under nitrogen gas then dialyzed against PBS using Slide-A-Lyzer (Thermo Fisher) dialysis cassettes overnight. The 20 mL of lipid-depleted FBS was sterilized through passage through a 0.2 μM filter prior to use. Twenty milliliters of lipid-depleted FBS was added to 500 mL of media supplemented with 1% penicillin−streptomycin.

Statistical Analysis. All results are displayed as mean ± SD. A minimum of three independent experiments (n = 3) having internal triplicates was performed for each result. Statistical analysis was performed in GraphPad Prism 8.3 using two-way ANOVA with a follow up Dunnett's test, p-value ≤0.05.

■ ASSOCIATED CONTENT

Supporting Information

The Supporting Information is available free of charge at https://pubs.acs.org/doi/10.1021/acsptsci.0c00207.

Figure S-1: OVCAR-8 and SKOV-3 spheroid morphology; Figure S-2: effects of compound treatment on OVCAR-8 and SKOV-3 spheroids; Figure S-3:effects of OSW-1 on ovarian cancer cells morphology and viability; Figure S-4: SKOV-3 spheroid development with 10% FBS; Figure S-5: cell imaging of ovarian cancer cells grown under lipid depleted conditions; Figure S-6: uncropped OSBP and ORP4 Western blots shown in

https://dx.doi.org/10.1021/acsptsci.0c00207
ACS Pharmacol. Transl. Sci. 2021, 4, 744−756

Figure 1D; Figure S-7: uncropped OSBP and ORP4 Western blots shown in Figure 5 (PDF)

AUTHOR INFORMATION

Corresponding Authors

Handan Acar − *Stephenson School of Biomedical Engineering and Stephenson Cancer Center, University of Oklahoma, Norman, Oklahoma 73019, United States*; Phone: (405) 325-2186; Email: hacar@ou.edu

Anthony W. G. Burgett − *Department of Chemistry and Biochemistry and Stephenson Cancer Center, University of Oklahoma, Norman, Oklahoma 73019, United States; Department of Pharmaceutical Sciences, University of Oklahoma Health Sciences Center, Oklahoma City, Oklahoma 73117, United States*; orcid.org/0000-0002-0685-5144; Phone: (405) 271-6592; Email: anthony-burgett@ouhsc.edu; Fax: (405) 271-7505

Authors

Ryan C. Bensen − *Department of Chemistry and Biochemistry, University of Oklahoma, Norman, Oklahoma 73019, United States*

Gokhan Gunay − *Stephenson School of Biomedical Engineering, University of Oklahoma, Norman, Oklahoma 73019, United States*

Matthew C. Finneran − *Department of Chemistry and Biochemistry, University of Oklahoma, Norman, Oklahoma 73019, United States*

Isha Jhingan − *Stephenson School of Biomedical Engineering, University of Oklahoma, Norman, Oklahoma 73019, United States*

Complete contact information is available at: https://pubs.acs.org/10.1021/acsptsci.0c00207

Author Contributions

#R.C.B. and G.G. made equal contributions as co-first authors.

Funding

This research was supported by funding from the National Institutes of Health (R21CA204706), the Oklahoma Center for Advancement of Science and Technology (OCAST) (HR17-116), IBEST-OUHSC, Oklahoma Tobacco Settlement Endowment Trust (TSET), and the Barnes Family Foundation (Tulsa, Oklahoma).

Notes

The authors declare no competing financial interest.

ACKNOWLEDGMENTS

We thank Dr. Zachary Severance for helpful edits in preparing this manuscript.

REFERENCES

(1) Torre, L. A., Trabert, B., DeSantis, C. E., Miller, K. D., Samimi, G., Runowicz, C. D., Gaudet, M. M., Jemal, A., and Siegel, R. L. (2018) Ovarian Cancer Statistics, 2018. *Ca-Cancer J. Clin. 68* (4), 284−296.

(2) Howlader, N., Noone, A., Krapcho, M., Noone, A., Neyman, N., Aminou, R., Altekruse, S., Kosary, C., Altekruse, S. F., and Kosary, C. L. (2012) SEER Cancer Statistics Review, 1975−2009.

(3) Lengyel, E. (2010) Ovarian Cancer Development and Metastasis. *Am. J. Pathol. 177* (3), 1053−1064.

(4) Armstrong, D. K., Bundy, B., Wenzel, L., Huang, H. Q., Baergen, R., Lele, S., Copeland, L. J., Walker, J. L., and Burger, R. A. (2006) Intraperitoneal Cisplatin and Paclitaxel in Ovarian Cancer. *N. Engl. J. Med. 354* (1), 34−43.

(5) Ahmed, N., and Stenvers, K. L. (2013) Getting to Know Ovarian Cancer Ascites: Opportunities for Targeted Therapy-Based Translational Research. *Front. Oncol. 3*, 256.

(6) Ishiguro, T., Ohata, H., Sato, A., Yamawaki, K., Enomoto, T., and Okamoto, K. (2017) Tumor-Derived Spheroids: Relevance to Cancer Stem Cells and Clinical Applications. *Cancer Sci. 108* (3), 283−289.

(7) Ahmed, N., Escalona, R., Leung, D., Chan, E., and Kannourakis, G. (2018) Seminars in Cancer Biology Tumour Microenvironment and Metabolic Plasticity in Cancer and Cancer Stem Cells: Perspectives on Metabolic and Immune Regulatory Signatures in Chemoresistant Ovarian Cancer Stem Cells. *Semin. Cancer Biol. 53*, 265−281.

(8) Göbel, A., Zinna, V. M., Dell'Endice, S., Jaschke, N., Kuhlmann, J. D., Wimberger, P., and Rachner, T. D. (2020) Anti-Tumor Effects of Mevalonate Pathway Inhibition in Ovarian Cancer. *BMC Cancer 20* (1), 1−17.

(9) Yang, J., and Stack, M. S. (2020) Lipid Regulatory Proteins as Potential Therapeutic Targets for Ovarian Cancer in Obese Women. *Cancers 12* (11), 1−25.

(10) Ji, Z., Shen, Y., Feng, X., Kong, Y., Shao, Y., Meng, J., Zhang, X., and Yang, G. (2020) Deregulation of Lipid Metabolism: The Critical Factors in Ovarian Cancer. *Front. Oncol. 10*, 1−10.

(11) Zheng, L., Li, L., Lu, Y., Jiang, F., and Yang, X. A. (2018) SREBP2 Contributes to Cisplatin Resistance in Ovarian Cancer Cells. *Exp. Biol. Med. 243* (7), 655−662.

(12) Couttenier, A., Lacroix, O., Vaes, E., Cardwell, C. R., De Schutter, H., and Robert, A. (2017) Statin Use Is Associated with Improved Survival in Ovarian Cancer: A Retrospective Population-Based Study. *PLoS One 12* (12), 1−14.

(13) Majidi, A., Na, R., Dixon-Suen, S., Jordan, S. J., and Webb, P. M. (2020) Common Medications and Survival in Women with Ovarian Cancer: A Systematic Review and Meta-Analysis. *Gynecol. Oncol. 157* (3), 678−685.

(14) Irvin, S., Clarke, M. A., Trabert, B., and Wentzensen, N. (2020) Systematic Review and Meta-Analysis of Studies Assessing the Relationship between Statin Use and Risk of Ovarian Cancer. *Cancer Causes Control 31* (10), 869−879.

(15) Zeybek, B., Costantine, M., Kilic, G. S., and Borahay, M. A. (2018) Therapeutic Roles of Statins in Gynecology and Obstetrics: The Current Evidence. *Reprod. Sci. 25* (6), 802−817.

(16) Elmore, R. G., Ioffe, Y., Scoles, D. R., Karlan, B. Y., and Li, A. J. (2008) Impact of Statin Therapy on Survival in Epithelial Ovarian Cancer. *Gynecol. Oncol. 111* (1), 102−105.

(17) Pampaloni, F., Reynaud, E. G., and Stelzer, E. H. K. (2007) The Third Dimension Bridges the Gap between Cell Culture and Live Tissue. *Nat. Rev. Mol. Cell Biol. 8* (10), 839−845.

(18) Nunes, A. S., Barros, A. S., Costa, E. C., Moreira, A. F., and Correia, I. J. (2019) 3D Tumor Spheroids as in Vitro Models to Mimic in Vivo Human Solid Tumors Resistance to Therapeutic Drugs. *Biotechnol. Bioeng. 116* (1), 206−226.

(19) Paullin, T., Powell, C., Menzie, C., Hill, R., Cheng, F., Martyniuk, C. J., and Westerheide, S. D. (2017) Spheroid Growth in Ovarian Cancer Alters Transcriptome Responses for Stress Pathways and Epigenetic Responses. *PLoS One 12* (8), No. e0182930.

(20) Goyeneche, A., Lisio, M.-A., Fu, L., Srinivasan, R., Valdez Capuccino, J., Gao, Z., and Telleria, C. (2020) The Capacity of High-Grade Serous Ovarian Cancer Cells to Form Multicellular Structures Spontaneously along Disease Progression Correlates with Their Orthotopic Tumorigenicity in Immunosuppressed Mice. *Cancers 12* (3), 699.

(21) Gunay, G., Kirit, H. A., Kamatar, A., Baghdasaryan, O., Hamsici, S., and Acar, H. (2020) The Effects of Size and Shape of the Ovarian Cancer Spheroids on the Drug Resistance and Migration. *Gynecol. Oncol. 159* (2), 563−572.

(22) Xing, H., Wang, S., Hu, K., Tao, W., Li, J., Gao, Q., Yang, X., Weng, D., Lu, Y., and Ma, D. (2005) Effect of the Cyclin-Dependent Kinases Inhibitor P27 on Resistance of Ovarian Cancer Multicellular

Spheroids to Anticancer Chemotherapy. *J. Cancer Res. Clin. Oncol. 131* (8), 511−519.
(23) Yang, Y., Li, S., Sun, Y., Zhang, D., Zhao, Z., and Liu, L. (2019) Reversing Platinum Resistance in Ovarian Cancer Multicellular Spheroids by Targeting Bcl-2. *OncoTargets Ther. 12*, 897−906.
(24) Tsubuki, M., Matsuo, S., and Honda, T. (2008) A New Synthesis of Potent Antitumor Saponin OSW-1 via Wittig Rearrangement. *Tetrahedron Lett. 49* (2), 229−232.
(25) Tang, Y., Li, N., Duan, J.-A., and Tao, W. (2013) Structure, Bioactivity, and Chemical Synthesis of OSW-1 and Other Steroidal Glycosides in the Genus Ornithogalum. *Chem. Rev. 113* (7), 5480−5514.
(26) Burgett, A. W. G., Poulsen, T. B., Wangkanont, K., Anderson, D. R., Kikuchi, C., Shimada, K., Okubo, S., Fortner, K. C., Mimaki, Y., Kuroda, M., et al. (2011) Natural Products Reveal Cancer Cell Dependence on Oxysterol-Binding Proteins. *Nat. Chem. Biol. 7* (9), 639−647.
(27) Roberts, B. L., Severance, Z. C., Bensen, R. C., Le, A. T., Kothapalli, N. R., Nuñez, J. I., Ma, H., Wu, S., Standke, S. J., Yang, Z., et al. (2019) Transient Compound Treatment Induces a Multigenerational Reduction of Oxysterol-Binding Protein (OSBP) Levels and Prophylactic Antiviral Activity. *ACS Chem. Biol. 14* (2), 276−287.
(28) Roberts, B. L., Severance, Z. C., Bensen, R. C., Le-McClain, A. T., Malinky, C. A., Mettenbrink, E. M., Nuñez, J. I., Reddig, W. J., Blewett, E. L., Burgett, A. W. G., et al. (2019) Differing Activities of Oxysterol-Binding Protein (OSBP) Targeting Anti-Viral Compounds. *Antiviral Res. 170*, 104548.
(29) Lim, C.-Y., Davis, O. B., Shin, H. R., Zhang, J., Berdan, C. A., Jiang, X., Counihan, J. L., Ory, D. S., Nomura, D. K., and Zoncu, R. (2019) ER-Lysosome Contacts Enable Cholesterol Sensing by MTORC1 and Drive Aberrant Growth Signalling in Niemann-Pick Type C. *Nat. Cell Biol. 21* (10), 1206−1218.
(30) Zhong, W., Xu, M., Li, C., Zhu, B., Cao, X., Li, D., Chen, H. H. H., Hu, C., Li, R., Luo, C., et al. (2019) ORP4L Extracts and Presents PIP2 from Plasma Membrane for PLCβ3 Catalysis: Targeting It Eradicates Leukemia Stem Cells. *Cell Rep. 26* (8), 2166−2177.
(31) Pietrangelo, A., and Ridgway, N. D. (2018) Bridging the Molecular and Biological Functions of the Oxysterol-Binding Protein Family. *Cell. Mol. Life Sci. 75* (17), 3079−3098.
(32) Antonny, B., Bigay, J., and Mesmin, B. (2018) The Oxysterol-Binding Protein Cycle: Burning Off PI(4)P to Transport Cholesterol. *Annu. Rev. Biochem. 87* (1), 809−837.
(33) Mesmin, B., Bigay, J., Moser von Filseck, J., Lacas-Gervais, S., Drin, G., and Antonny, B. (2013) A Four-Step Cycle Driven by PI(4)P Hydrolysis Directs Sterol/PI(4)P Exchange by the ER-Golgi Tether OSBP. *Cell 155* (4), 830−843.
(34) Strating, J. R. P. M., van der Linden, L., Albulescu, L., Bigay, J., Arita, M., Delang, L., Leyssen, P., van der Schaar, H. M., Lanke, K. H. W., Thibaut, H. J., et al. (2015) Itraconazole Inhibits Enterovirus Replication by Targeting the Oxysterol-Binding Protein. *Cell Rep. 10* (4), 600−615.
(35) Zhong, W., Yi, Q., Xu, B., Li, S., Wang, T., Liu, F., Zhu, B., Hoffmann, P. R., Ji, G., Lei, P., et al. (2016) ORP4L Is Essential for T-Cell Acute Lymphoblastic Leukemia Cell Survival. *Nat. Commun. 7*, 12702.
(36) Charman, M., Colbourne, T. R., Pietrangelo, A., Kreplak, L., and Ridgway, N. D. (2014) Oxysterol-Binding Protein (OSBP)-Related Protein 4 (ORP4) Is Essential for Cell Proliferation and Survival. *J. Biol. Chem. 289* (22), 15705−15717.
(37) Moreira, E. F., Jaworski, C., Li, a, and Rodriguez, I. R. (2001) Molecular and Biochemical Characterization of a Novel Oxysterol-Binding Protein (OSBP2) Highly Expressed in Retina. *J. Biol. Chem. 276* (21), 18570−18578.
(38) Udagawa, O., Ito, C., Ogonuki, N., Sato, H., Lee, S., Tripvanuntakul, P., Ichi, I., Uchida, Y., Nishimura, T., Murakami, M., et al. (2014) Oligo-Astheno-Teratozoospermia in Mice Lacking ORP4, a Sterol-Binding Protein in the OSBP-Related Protein Family. *Genes to Cells 19* (1), 13−27.
(39) Cao, X., Chen, J., Li, D., Xie, P., Xu, M., Lin, W., Li, S., Pan, G., Tang, Y., Xu, J., et al. (2019) ORP4L Couples IP 3 to ITPR1 in Control of Endoplasmic Reticulum Calcium Release. *FASEB J. 33* (12), 13852−13865.
(40) Li, J., Xiao, Y., Lai, C., Lou, N., Ma, H., Zhu, B.-Y., Zhong, W.-B., and Yan, D.-G. (2016) Oxysterol-Binding Protein-Related Protein 4L Promotes Cell Proliferation by Sustaining Intracellular Ca^{2+} Homeostasis in Cervical Carcinoma Cell Lines. *Oncotarget 7* (40), 65849.
(41) Garcia-Prieto, C., Riaz Ahmed, K. B., Chen, Z., Zhou, Y., Hammoudi, N., Kang, Y., Lou, C., Mei, Y., Jin, Z., and Huang, P. (2013) Effective Killing of Leukemia Cells by the Natural Product OSW-1 through Disruption of Cellular Calcium Homeostasis. *J. Biol. Chem. 288* (5), 3240−3250.
(42) Uhlén, M., Fagerberg, L., Hallström, B. M., Lindskog, C., Oksvold, P., Mardinoglu, A., Sivertsson, Å., Kampf, C., Sjöstedt, E., and Asplund, A. (2015) Tissue-Based Map of the Human Proteome. *Science (Washington, DC, U. S.) 347* (6220), 1260419.
(43) Zhou, Y., Garcia-Prieto, C., Carney, D. a, Xu, R. -h., Pelicano, H., Kang, Y., Yu, W., Lou, C., Kondo, S., Liu, J., et al. (2005) OSW-1: A Natural Compound With Potent Anticancer Activity and a Novel Mechanism of Action. *JNCI J. Natl. Cancer Inst. 97* (23), 1781−1785.
(44) Domcke, S., Sinha, R., Levine, D. A., Sander, C., and Schultz, N. (2013) Evaluating Cell Lines as Tumour Models by Comparison of Genomic Profiles. *Nat. Commun. 4* (1), 2126.
(45) Nigjeh, S. E., Yeap, S. K., Nordin, N., Kamalideghan, B., Ky, H., and Rosli, R. (2018) Citral Induced Apoptosis in MDA-MB-231 Spheroid Cells. *BMC Complementary Altern. Med. 18* (1), 56.
(46) Alimperti, S., Lei, P., Wen, Y., Tian, J., Campbell, A. M., and Andreadis, S. T. (2014) Serum-Free Spheroid Suspension Culture Maintains Mesenchymal Stem Cell Proliferation and Differentiation Potential. *Biotechnol. Prog. 30* (4), 974−983.
(47) Amaral, R. L. F., Miranda, M., Marcato, P. D., and Swiech, K. (2017) Comparative Analysis of 3D Bladder Tumor Spheroids Obtained by Forced Floating and Hanging Drop Methods for Drug Screening. *Front. Physiol. 8*, 1 DOI: 10.3389/fphys.2017.00605.
(48) Criscuolo, D., Avolio, R., Calice, G., Laezza, C., Paladino, S., Navarra, G., Maddalena, F., Crispo, F., Pagano, C., Bifulco, M., et al. (2020) Cholesterol Homeostasis Modulates Platinum Sensitivity in Human Ovarian Cancer. *Cells 9* (4), 828.
(49) Hannah, V. C., Ou, J., Luong, A., Goldstein, J. L., and Brown, M. S. (2001) Unsaturated Fatty Acids Down-Regulate Srebp Isoforms 1a and 1c by Two Mechanisms in HEK-293 Cells. *J. Biol. Chem. 276* (6), 4365−4372.
(50) Adams, C. M., Reitz, J., De Brabander, J. K., Feramisco, J. D., Li, L., Brown, M. S., and Goldstein, J. L. (2004) Cholesterol and 25-Hydroxycholesterol Inhibit Activation of SREBPs by Different Mechanisms, Both Involving SCAP and Insigs. *J. Biol. Chem. 279* (50), 52772−52780.
(51) Hirst, J., Pathak, H. B., Hyter, S., Pessetto, Z. Y., Ly, T., Graw, S., Koestler, D. C., Krieg, A. J., Roby, K. F., and Godwin, A. K. (2018) Licofelone Enhances the Efficacy of Paclitaxel in Ovarian Cancer by Reversing Drug Resistance and Tumor Stem-like Properties. *Cancer Res. 78* (15), 4370−4385.
(52) Pan, G., Cao, X., Liu, B., Li, C., Li, D., Zheng, J., Lai, C., Olkkonen, V. M., Zhong, W., and Yan, D. (2018) OSBP-Related Protein 4L Promotes Phospholipase Cβ3 Translocation from the Nucleus to the Plasma Membrane in Jurkat T-Cells. *J. Biol. Chem. 293* (45), 17430−17441.
(53) Guillaumond, F., Bidaut, G., Ouaissi, M., Servais, S., Gouirand, V., Olivares, O., Lac, S., Borge, L., Roques, J., Gayet, O., et al. (2015) Cholesterol Uptake Disruption, in Association with Chemotherapy, Is a Promising Combined Metabolic Therapy for Pancreatic Adenocarcinoma. *Proc. Natl. Acad. Sci. U. S. A. 112* (8), 2473−2478.
(54) Wang, W., Bai, L., Li, W., and Cui, J. (2020) The Lipid Metabolic Landscape of Cancers and New Therapeutic Perspectives. *Front. Oncol. 10*, 1−15.

(55) Casella, C., Miller, D. H., Lynch, K., and Brodsky, A. S. (2014) Oxysterols Synergize with Statins by Inhibiting SREBP-2 in Ovarian Cancer Cells. *Gynecol. Oncol. 135* (2), 333−341.
(56) Riss, T., Valley, M., Kupcho, K., Zimprich, C., Leippe, D., Niles, A., Vidugiriene, J., Cali, J., Kelm, J., Moritz, W., et al. (2014) Validation of in Vitro Assays to Measure Cytotoxicity in 3D Cell Cultures. *Toxicol. Lett. 229* (229), S145.
(57) Kijanska, M., and Kelm, J. (2004) *In Vitro 3D Spheroids and Microtissues: ATP-Based Cell Viability and Toxicity Assays*; Eli Lilly & Company and the National Center for Advancing Translational Sciences.

https://dx.doi.org/10.1021/acsptsci.0c00207
ACS Pharmacol. Transl. Sci. 2021, 4, 744−756